—研究論文—
Scientific Paper

Characteristics of the natural remanent magnetization (NRM) of a core collected from offshore Wilkes Land, East Antarctica

Haruka Matsuoka[1] and Minoru Funaki[2]

東南極ウィルクスランド沖深海底堆積物の自然残留磁化の特性

松岡東香[1]・船木　實[2]

(Received September 8, 2003; Accepted September 24, 2003)

要旨: 東南極ウィルクスランド沖から採取された深海底堆積物の自然残留磁化（NRM）の特性を明らかにするため，古地磁気・岩石磁気実験が行われた．コア長は540 cmである．すべての試料に対し，5 mTから100 mTまでの段階交流消磁実験を行った．本試料は，他地域における一般的な堆積物の10倍から100倍ものNRM強度を示した．コアの上部460 cmでは，大部分の試料が一つの安定な残留磁化成分を持っており，100 mTの交流磁場でも消磁できない特異な高安定成分の存在が確認された．これに対し，コア下部では二次磁化を獲得して不安定な消磁曲線を描く試料が多く存在した．全試料に対し詳細な消磁実験を行ったところ，すべての試料の二次磁化が30 mTの交流磁場で殆ど消去されていることから，最適消磁レベルは30 mTと推定された．最適消磁レベルで消磁したNRMは，本コア試料が三つの地磁気極性を含んでいることを明らかにした．さらに，古地磁気測定に1 ccの小型立方サンプルを用いることにより，古地磁気記録の時間分解能を大きく向上させることに成功した．非履歴性残留磁化（ARM）の獲得及び消磁実験を行ったところ，すべての試料が安定なARMを獲得し，その強度もコア一貫して変動が小さいことを確認できた．これは，不安定な残留磁化成分のみを持つ試料が，弱い地球磁場中で残留磁化を獲得した可能性を示唆するものである．

Abstract: Paleomagnetic and rockmagnetic studies were carried out in order to investigate the characteristics of natural remanent magnetization (NRM) of deep-sea sediments cored from offshore Wilkes Land, East Antarctica. The core is 540 cm long. Alternating-field (AF) demagnetization experiments using a stepwise AF field from 5 to 100 mT were conducted on all of the samples. The NRM intensities are 10–100 times higher than those commonly obtained from different localities. In the upper 460 cm of the core, most samples had stable single component magnetization, and remarkable high-stability components which survived up to 100 mT were observed. In the lower section of the core, in contrast, many samples showed more unstable (zigzag) demagnetization curves and secondary acquired magnetizations. The optimum AF demagnetization field intensity was assumed to be 30 mT, because the secondary magnetizations of every sample seemed to be completely demagnetized at

[1] 総合研究大学院大学数物科学研究科極域科学専攻. Department of Polar Science, School of Mathematical and Physical Science, The Graduated University for Advanced Studies, National Institute of Polar Research, Kaga 1-chome, Itabashi-ku, Tokyo 173–8515.

[2] 国立極地研究所. National Institute of Polar Research, Kaga 1-chome, Itabashi-ku, Tokyo 173–8515.

南極資料, Vol. 47, No. 3, 315–327, 2003
Nankyoku Shiryô (Antarctic Record), Vol. 47, No. 3, 315–327, 2003

that AF field. The down core NRM variation after demagnetization by the optimum field revealed that the core contains 3 polarity intervals. By using smaller cubic samples of 1 cc volume, the time resolution of the paleomagnetic record was much improved. Anhysteretic remanent magnetization (ARM) experiments were also conducted on all of the samples. The results of the AF demagnetization of ARM imply that the samples showing only soft NRM component possibly acquired their magnetization under a weak geomagnetic field.

1. Introduction

Deep-sea sediments provide continuous records of the past geomagnetic field, and numerous paleomagnetic studies, using sedimentary sequences, have been done to investigate the behavior of Earth's magnetic field in the past. However, the number of paleomagnetic records from the Antarctic regions, involving both direction and intensity of geomagnetic field for over 1 Ma, still seems to be small, as compared with those from other regions. For understanding of the evolution of the global-scale geomagnetic field, it is essential to obtain continuous paleomagnetic records from the Antarctic regions.

In the Antarctic region, several magnetostratigraphic studies have been done (*e.g.*, Sakai *et al.*, 1990; Keating and Sakai, 1991; Sakai and Keating, 1991; Inokuchi and Heider, 1992; Florindo *et al.*, 2003). Though their paleomagnetic records span over a million years, such records possibly contain many fragments and their time resolutions are insufficient for studying geomagnetic field behavior in many cases. Brachfeld *et al.* (2000) did a paleomagnetic study on five sedimentary sequences cored in the western margin of the Antarctic Peninsula. The two cores were collected by the United States Antarctic Program (USAP), while the other three were cored during the Ocean Drilling Program (ODP) Leg 178. They conducted paleomagnetic measurements on these cores and evaluated their inclination records to determine the discrepancies between split-core and U-channel measurements from the same core. In that study, a single continuous record of inclination and relative paleointensity over the past 9000 yr was obtained as the first high-resolution record of paleosecular variation for the Antarctic Peninsula region. Guyodo *et al.* (2001) provided a paleomagnetic record for a part of the Matuyama Chron, derived from sediments collected from drift deposits off the Western Antarctic Peninsula continental margin, at ODP Site 1101 (Leg 178). The inclination record over the time interval 0.7–2.1 Ma, the relative paleointensity record over the 0.7–1.1 Ma interval and a comparison with eight other paleointensity records over the 0.95–1.1 Ma interval were reported. They constructed a composite record of relative paleointensity for the Jaramillo subchron with nine records from different oceans in the study. Sagnotti *et al.* (2001) investigated the climatically induced magnetic mineralogy changes on three cores obtained from a hemipelagic sediment drift on the continental rise of the Pacific margin of the Antarctic Peninsula during the Sediment Drifts of the Antarctic Offshore (SEDANO) project (Lucchi *et al.*, 2002). They obtained inclination records, relative paleointensity records and rock magnetic data spanning the last 160 kyr. Escutia *et al.* (2003) performed paleomagnetic measurements on several cores collected across the eastern part of the Antarctic Wilkes Land margin during the Deep Freeze 79 cruise (Domack, 1982) and the United States Geological Survey 1984 cruise (Hampton *et al.*, 1987a, b). However, their paleomagnetic data are available only for magnetostratigraphy; they are not sufficient for the study of paleosecular variation, since the study was directed at understanding the age and process of sedimentation across the margin. They collected 6–12 discrete samples at 15–20 cm intervals from each of the five cores and measured their inclinations. Nevertheless, the one core yielded continuous inclination and declination data using U-channel samples; low sedimentation rates of around 0.01 cm/kyr and the presence of hiatuses limited the time resolution of their data.

The core used in this study was collected on the TH94 cruise (1994–1995) of R/V *Hakurei-maru*, carried out by the Technology Research Center, Japan National Oil Corporation (Ishihara *et al.*, 1996). A fundamental paleomagnetic study of this core was performed by Sakai *et al.* (1998) using discrete samples of 7 cc collected from one side of the core divided in half. They applied AF demagnetization up to 80 mT in 5 mT steps in order to identify the optimum demagnetization level only for several pilot samples, whereas demagnetization was done up to 30 mT with few steps on the residual samples. However, such demagnetizations performed only on pilot samples might be insufficient to determine how large soft (secondary) magnetization was acquired by all of the samples. In this study, we studied the stability of the natural remanent magnetization (NRM) based on the AF demagnetizations of NRM and investigated the ability of the sediments to acquire magnetization based on anhysteretic remanent magnetization (ARM) experiments, using the other side of the core (archived halves of cores).

According to Sakai *et al.* (1998), the average sedimentation rate of this core was very slow, about 5 mm/kyr. The low sedimentation rate severely restricts the time resolution of paleomagnetic data. However, sediments deposited slowly in an oxidized environment, can provide a paleomagnetic record of high reliability, because the magnetic minerals in such sediments presumably suffer less alteration in early diagenesis than those in reduced sediments deposited at a high sedimentation rate (*e.g.*, Yamazaki, 1999). In our case, the paleomagnetic record derived from 7 cc samples is likely to suffer from the time-averaging effect caused by the thickness of samples, though 7 cc samples are most commonly used as discrete samples in various paleomagnetic studies. Kawai *et al.* (1976) and Sato and Kobayashi (1989) succeeded in obtaining high time resolution records by using thin sections of $2.4 \times 2.4 \times 0.43$ cm. For investigating both declination and inclination, however, the magnetic measurements using cubic-shaped samples should be much preferable. Thus we performed the magnetic measurements by employment of 1 cc cubic samples in order to obtain a higher time resolution record.

2. Geological setting and sampling

The Wilkes Land continental margin formed by the breakup of Australia and Antarctica, which was estimated at 55 Ma on the basis of magnetic anomaly patterns by Weissel and Hayes (1972), was estimated at 90–112 Ma in subsequent revision of the anomaly interpretations by Cande and Mutter (1982) and at 95 ± 5 Ma by Veevers (1987). From the eastern part of the Wilkes Land margin, a number of geophysical and geological data have been reported (*e.g.*, Tanahashi *et al.*, 1987; Eittreim and Smith, 1987; Hampton *et al.*, 1987a, b; Eittreim *et al.*, 1995); in contrast, only a few have been obtained from the western part of the Wilkes Land margin (*e.g.*, Hayes *et al.*, 1975; Tsumuraya *et al.*, 1985; Ishihara *et al.*, 1996). In the vicinity of our study area, Hayes *et al.* (1975) reported the lithology of the sequence cored from about 3500 m deep at site 268 (63° 56.99′S, 105° 09.34′E) of the Deep Sea Drilling Project (DSPS). The coring site is depicted in Fig. 1. They divided the core of 474 m into three units as shown in Table 1. The site has experienced dominantly terrigenous sedimentation and the sediments are chiefly silty clays with the transition from diatom-bearing or diatom-rich above, to nanofossil-rich below (Hayes *et al.*, 1975; Kemp *et al.*, 1975). Other geological and geophysical data from the western part of Wilkes Land margin were obtained from Tsumuraya *et al.* (1985) and Ishihara *et al.* (1996).

The core used in this study was obtained from a continental rise site 3060 m deep at the western part of the Antarctic Wilkes Land margin. The core was collected with a gravity corer. The position of the coring site is 63° 43.13′S, 112° 20.06′E (Fig. 1). The total length of the core is 540 cm. The surface sediments, at least 20 cm, were lost while recovering. The core was estimated to have been collected perpendicularly, while the north direction of the core was unknown. Subsequently the core was separated into 6 sub-cores (numbers: 1 to 5 and C) of 1 m length keeping their orientations and was split in half lengthwise. They were then sealed in split core shaped plastic cases and stored at 5 degrees centigrade to minimize dehydration of the sediments.

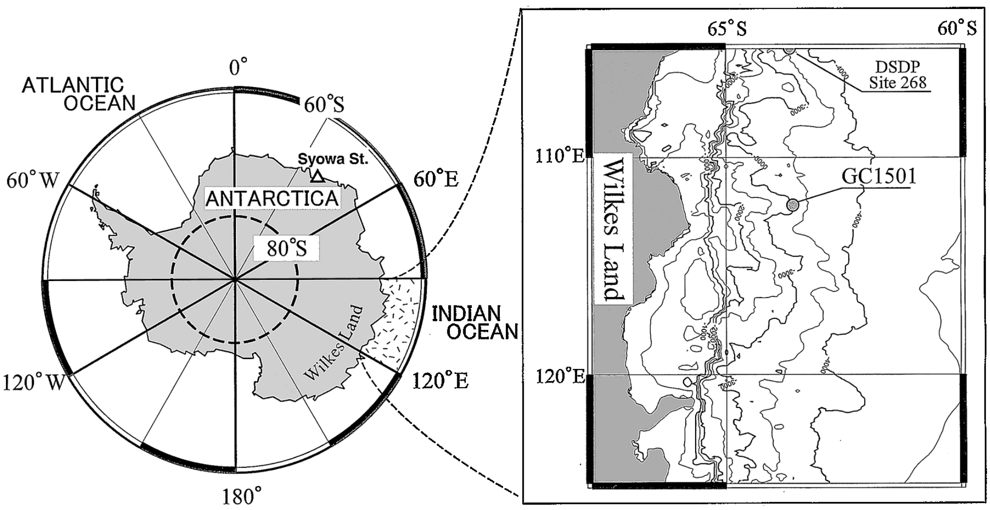

Fig. 1. Map showing the coring site (63° 43.13′S, 112° 20.06′E).

Table 1. Lithologic Units, DSDP Site 268 (Hayes et al., 1975).

Unit	Lithology	Subbotom depth (m)	Unit thickness (m)	Age
1	Clay, silty clay, sand, and diatom ooze	0–∼160	∼161	Pliocene to Quarternary
2	Clay, silty clay, sand, and nano ooze	∼160–228	∼68	Early Miocene
3	Silty clay, laminated silty clay and clayey silt, and chert	228–>474.5	∼256.5	Mid-Oligocene or older to Early Miocene

The 236 discrete samples of 7 cc (edge length is 2.3 cm) and 436 discrete samples of 1 cc (edge length is 1.2 cm) were sequentially taken from the archive halves of sub-cores in August 2001. All the samples were then sealed to minimize dehydration of the sediments.

The sediment material was siliceous silt of brownish gray color. Abundant foraminiferal skeletons in good preservation were observed throughout the core. Paleoclimatically induced lithological variations were not observed. This implies that the sediment was deposited in an environmentally stable condition.

3. Measurements

3.1. AF demagnetization of NRM using 7 cc samples

The magnetic instrument used in this study was a SQUID magnetometer with a static three-axis alternating AF demagnetizer and an ARM acquisition coil, which was produced by 2G Enterprises. The magnetometer is installed in a low magnetic field room in the National Institute of Polar Research in Tokyo, Japan. All samples were demagnetized up to 100 mT in steps of 5 mT. The representative AF demagnetization curves described by Zijderveld projections are shown in Fig. 2. In general, almost all samples from the surface to 460 cm depth have very stable NRM as shown in Fig. 2(a); the NRM of sample 1-M11 (23.8 cm) was gradually demagnetized linearly toward the coordinate axes for both the vertical and horizontal components. The NRM of these samples were on the order of 10^{-2} A/m in intensity and were magnetized to the normal polarity (upward). In the lower section of the core, in contrast, many samples showed more unstable (zigzag) demagnetization curves. The demagnetization curve of sample 5-M28 (462.0 cm) showed at least 2 component magnetizations, as shown in Fig. 2(b). The soft component of the normal polarity was demagnetized to 20 mT, while the hard component of the reversed polarity seemed to survive up to 100 mT. The intensity was more than 10 times weaker than that of the sample 1-M11. A similar demagnetization curve and intensities appeared in sample C-M07, as shown in Fig. 2(c), while the

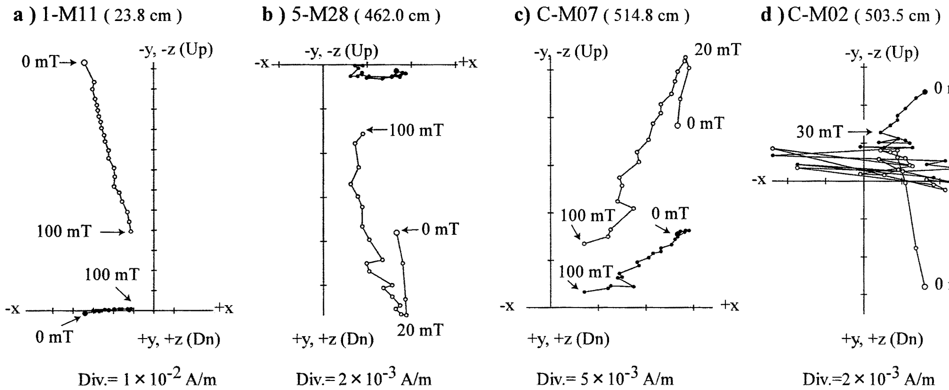

Fig. 2. Representative results of progressive AF demagnetization of specimens. Solid/open circles show projections on the horizontal/vertical plane.

polarities were opposite for the hard and soft components. However, a few samples showed only soft NRM components as shown in Fig. 2(d). The NRM was demagnetized linearly up to 30 mT, but it underwent drastic zigzag variations. The NRM intensity of this sample was on the order of 10^{-3} A/m. The linear demagnetization between 0 and 30 mT is due to only the soft component. Throughout the demagnetization curves, the optimum AF demagnetization field intensity was inferred to be 30 mT, because the soft NRM components of every sample seemed to be demagnetized completely before 30 mT.

The AF demagnetization curves of the normalized NRM intensities are shown in Fig. 3 for the representative 6 samples (sample numbers and depths are given in the figure) collected from each core. The unusual almost straight demagnetization curves (samples 1-M11, 2-M04, 3-M06 and 4-M10) appeared for the samples from up to 460 cm depth. The intensities of the other 2 samples (5-M28 and C-M07) collected from lower locations than that depth increased up to 20 mT and then decreased gradually due to the overprints of the normal and reversed NRM components. The residual NRM intensities after AF demagnetization to 100 mT were 23–32% of their original intensities. The median destructive field (MDF) was in the range of 58.6–81.6 mT (average 71.8 mT). These tendencies of the residual NRM and MDF values were consistent throughout the samples.

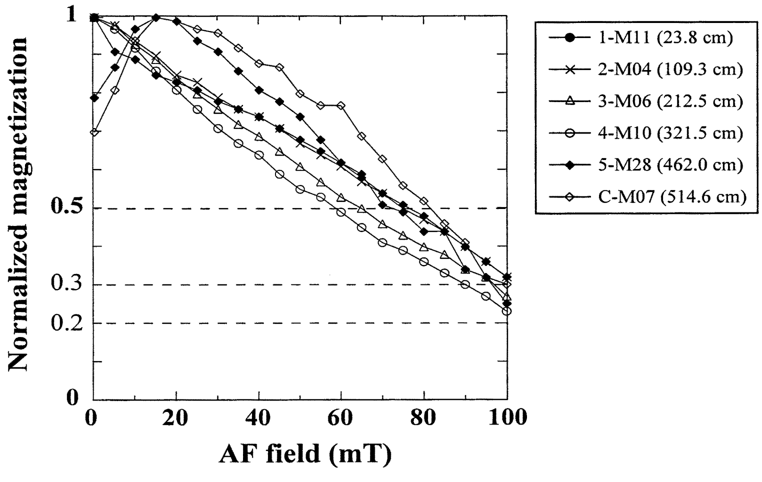

Fig. 3. NRM intensity decay plots in AF demagnetization.

3.2. AF demagnetization of ARM using 7 cc samples

ARM was imparted on the every sample by superimposing a DC biasing field of 0.1 mT on a smoothly decreasing AF field with a peak of 100 mT, and then ARM was AF demagnetized up to 100 mT. Since our cores were obtained from the Antarctic polar region, the dominant NRM component is vertical, as supported by the AF demagnetization results (Fig. 2), and it was not demagnetized completely for almost all cores even if the demagnetization field was 100 mT (Figs. 2, 3). Therefore, ARM was imparted toward the horizontal direction of the core to minimize the effect of the residual NRM after the demagnetization.

The AF demagnetization curves of ARM (magnetized toward the $+y$ axis) described in the Zijderveld projections are shown in Fig. 4 for samples 1-M11 and C-M 02. The former sample had only stable NRM, while the latter one had relatively unstable NRM as shown in Fig. 2 (a and d). The respective ARM intensities 8.56×10^{-2} and 9.88×10^{-2} A/m were not so different and the curves showed almost the same demagnetization. During the demagnetization of the ARM, the directions of the ARM components did not shift by 100 mT in either of the samples. From these viewpoints, it can be concluded that very stable and almost equal ARM intensities were acquired by both samples.

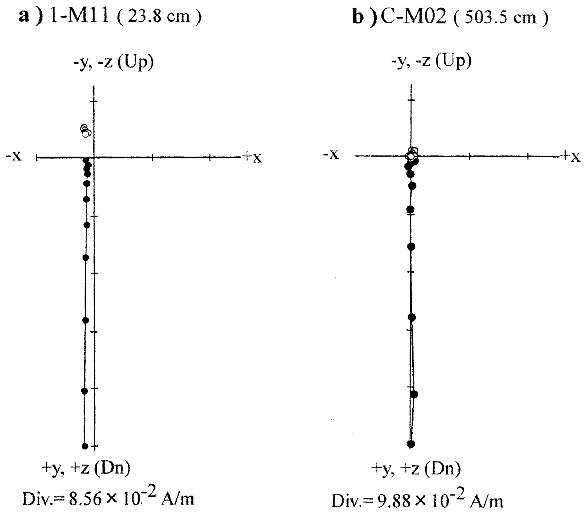

Fig. 4. Examples of stepwise AF demagnetization of ARM. Solid/open circles show projections on the horizontal/vertical plane.

3.3. Downcore variation of NRM using 7 cc samples

The downcore NRM variation after demagnetization by the optimum field (30 mT) was obtained by using 7 cc samples (Fig. 5). The intensity change curve shows four large peaks with 1.47×10^{-1} A/m (70 cm depth) for the maximum intensity in the upper 460 cm and remarkably small values with 9.10×10^{-4} A/m (473 cm depth) for the minimum intensity below the upper region. The declination curve shows relatively small zigzag changes around the zero declination line (relative declination) up to 460 cm, but the amplitudes of the variation are much larger below that depth. The inclination change curve was almost stabilized at -76.7 degrees with small variations up to 460 cm, but it shifted suddenly to about $+74.5$ degrees at 460 cm and changed again to -62.9 degrees at 510 cm. The drastically changed declination and inclination curves seem to be synchronized with each other, where the change occurred at 460 cm for the first one, 504 cm for the second one and 526 cm for the third one.

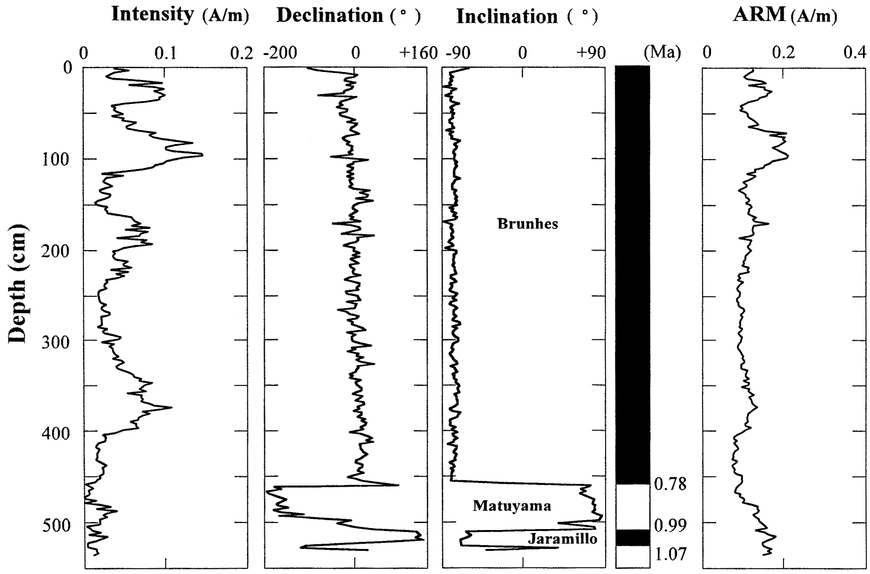

Fig. 5. Downcore variations of the NRM intensity, direction and ARM intensity after AF demagnetization at 30 mT with the magnetostratigraphy of Cande and Kent (1995). The declinations are relative because the core was not azimuthally oriented. The profiles were obtained by using 7 cc samples.

3.4. *Downcore variation of NRM using 1 cc samples*

The downcore NRM variation after demagnetization by the optimum field (30 mT) was obtained by using 1 cc samples (Fig. 6). The intensity curve exhibits high-frequency oscillations of small amplitudes and four large peaks with 1.34×10^{-1} A/m (97 cm depth) for the maximum intensity, while remarkably small values appears in the lower 460 cm depth. The declination curve exhibits high-frequency oscillations around the zero declination line (relative declination) up to 460 cm. The higher amplitude fluctuations in the declination curve appear at 11, 31, 167, 319, 338 and 395 cm in the part of upper part than that depth. The reliabilities of the fluctuations at 319 cm and 338 cm might be insufficient, because the inclinations at those depths are fairly high (-85.9 degrees for 319 cm and -87.7 degrees for 338 cm). The inclination change curve was almost stabilized between -58.5 and -89.1 degrees (average: -77.2 degrees) with small but high-frequency variations up to 455 cm. Sets of large-amplitude oscillations occur lower than that depth in both the declination and inclination curves.

3.5. *Downcore variation of ARM*

The downcore variations of ARM intensities after demagnetization by the optimum field (30 mT) were obtained by using 7 cc samples (Fig. 5) and 1 cc samples (Fig. 6). The two variations agree well with each other, though the ARM curve obtained from 1 cc samples shows higher-frequency oscillations than the variation obtained from 7 cc samples. Both curves exhibit humps at about 30 cm and 90 cm, and depict depression in the lower section between 405 and 460 cm. The average value of ARM is 0.12 A/m

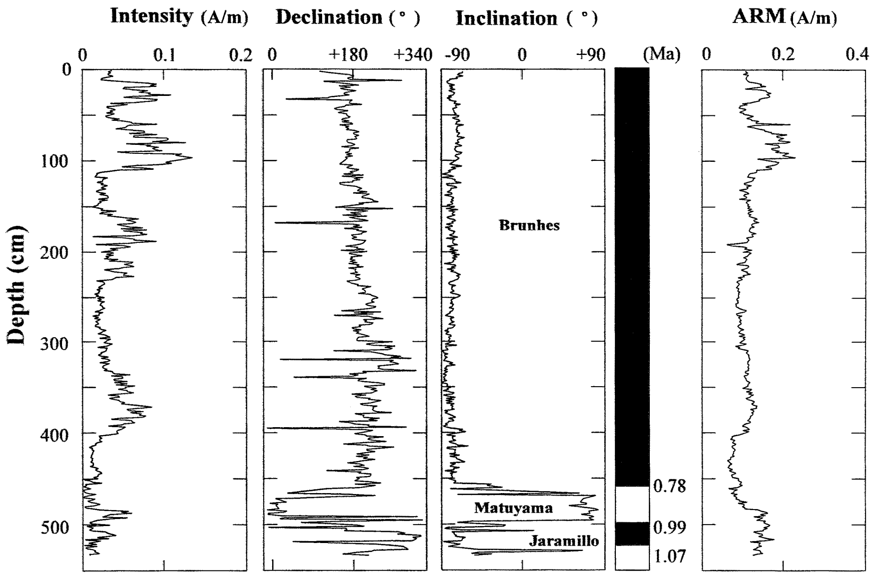

Fig. 6. Downcore variations of the NRM intensity, direction and ARM intensity after AF demagnetization at 30 mT with the magnetostratigraphy of Cande and Kent (1995). The declinations are relative because the core was not azimuthally oriented. The profiles were obtained by using 1 cc samples.

in both variations. The ARM curve obtained from 7 cc samples varies from a minimum of 0.07 A/m to a maximum of 0.21 A/m, while the ARM curve obtained from 1 cc samples does from a minimum of 0.06 A/m to a maximum of 0.23 A/m.

4. Discussion

The NRM intensities are 10–100 times higher than those commonly obtained from different localities, though such high values are sometimes reported from mid or high latitudes (*e.g.*, Channel *et al.*, 1997; Guyodo *et al.*, 2001). The unusual straight demagnetization curves (Fig. 3) observed in many samples indicate that each sample has a fairly flat distribution of coercivity of NRM carrier grains. The high coercive components of NRM have never been demagnetized completely as the residual NRM of 23–32% can survive, even if the samples are demagnetized up to 100 mT (Fig. 3). The high MDF value of average 71.8 mT also suggests remarkably high stability of NRM.

The downcore NRM variations obtained from the 7 cc and 1 cc samples, in general, showed coincident changes with each other (Figs. 5, 6), though the higher amplitudes of oscillations in declination and inclination curves and the much shorter-term changes appear in variations obtained from 1 cc samples. Significant switching fluctuations of high amplitude were observed in both declination and inclination curves of 1 cc samples below 455 cm, which have never been detected using 7 cc samples. Such results are possibly attributed to the time-averaging effect caused by the thickness of 7 cc cubes.

The two downcore variations of ARM, the one obtained by using 7 cc samples and the other by using 1 cc samples, show good agreement in their trends of intensity variations, average values, maxima and minima despite the difference of frequencies of their oscillations. The ARM varies only by a factor of 2.9 (maximum/minimum of ARM intensities) in the former variation and by a factor of 3.6 in the latter one, which shows that the ability of the sediments to acquire magnetization might not differ much overall.

The ARM intensities and AF demagnetization curve of the ARM suggest that the samples 1-M11 and C-M02 have the same magnetic characteristics as the stable and strong ARM. Namely, both samples are able to have stable NRM. However, the NRM stabilities of these samples were quite different; the former magnetized stable NRM but the latter was unstable. This difference can be explained by assuming that the former sample acquired the NRM under a reasonably strong geomagnetic field, while the latter acquired it in a rather weak that field.

The brownish gray color of the core is inferred to be strongly oxidized sediment. It is supported by the presence of foraminiferal skeletons consisting of Ca, because in the reduced condition such Ca rich fossils should disappear. Such a condition might imply the presence of iron oxide minerals as the dominant magnetic carrier. The absence of color variations in the core, the ARM demagnetization properties of the stable NRM sample and the unstable sample (Fig. 4), and the downcore variations of ARM imply that the magnetic carrier minerals may not be so different throughout the core.

The normal and reversed polarities of NRM after AF demagnetization to 30 mT can be compared with the magnetostratigraphy of Cande and Kent (1995). The most plausible fitting of the inclination and declination profiles derived by using 7 cc samples is represented in Fig. 5; from the surface to 460 cm depth for Brunhes Chron, from lower than 460 cm for Matuyama Chron and 504 to 526 cm for Jaramillo Subchron. In profiles from measurements using 1 cc samples (Fig. 6), however, the upper and lower boundaries of the Jaramillo Subchron seem to be defined at 495 cm and 527 cm. Because of its higher time resolution, the results using 1 cc samples should be preferred over the results using 7 cc samples. Those boundaries of the Chron and Subchron are assigned to 0.78, 0.99 and 1.07 Ma respectively. Sakai *et al*. (1998) showed the downcore variations of inclination after AF demagnetization at 30 mT, and suggested the negative high inclination up to 460 cm depth, and subsequently positive and negative ones. Our profiles of the inclination and declination (Figs. 5, 6), also demagnetized by 30 mT, are generally consistent with their results. As the soft NRM component VRM was completely demagnetized, the reliability of NRM seems to be enough. Therefore, the similarity of these profiles strongly suggests that the NRM is uniform at the same level of both split cores.

This magnetostratigraphy suggests that the core recorded geomagnetic secular variations up to 1.07 Ma. It is consistent with Sakai *et al*. (1998), but the reliability of NRM was much improved. As the NRM intensity profile (Fig. 5) used only stable NRM components, the variation should be reflected in the amount of the magnetic grains and intensity of the geomagnetic field. The amount of magnetic minerals might not vary throughout the core, estimated by the downcore variations of ARM intensities (Figs. 5, 6). Therefore, the very low NRM intensities observed in the Matuyama Chron seem to be attributed to the weak geomagnetic field, though such a result has been reported by only a few studies (*e.g.,* Sakai *et al*., 1998; Guyodo *et al*., 2001). Otherwise, the drastic change of the magnetic minerals and/or their grain sizes possibly occurred around the Brunhes/Matuyama boundary.

5. Conclusions

We investigated the characteristics of the NRM of a sedimentary sequence obtained from offshore Wilkes Land. In order to obtain high time resolution data from the core, the magnetic measurements were performed using not only 7 cc samples but also 1 cc small samples. The downcore variations obtained from 7 cc samples and those obtained from 1 cc samples agreed well with each other, while the higher oscillation amplitudes and shorter-term changes appeared in the variations obtained by using 1 cc samples. The AF demagnetization of NRM revealed that the sediments have fairly stable NRM components and the soft components of NRM were perfectly demagnetized by a 30 mT AF field. The remarkably high values of NRM intensity, the unusual straight demagnetization curves and the high-stability components which survived up to 100 mT, were observed. The ARM was stable and only small changes were observed in its downcore variations, which indicate that the ability of the sediments to acquire magnetization does not so differ overall. Thus the samples showing only soft NRM components possibly acquired their magnetization under a weak geomagnetic field. Our downcore NRM variations were mostly consistent with Sakai *et al*. (1998), but the time resolution of the paleomagnetic record was much improved by employment of 1 cc samples. Since the stability of NRM was proved in this study and the magnetostratigraphy showed that the core recorded geomagnetic secular variations up to 1.07 Ma, further investigation should be done for paleointensity estimates with this core.

Acknowledgments

We are grateful to the scientists, officers, and crew on the TH94 cruise of R/V *Hakurei-maru* for obtaining the core used in this study, and the Japan National Oil Corporation for providing the core. We also thank Takaharu Sato for his useful suggestions and discussions.

References

Brachfeld, S., Acton, G.D., Guyodo, Y. and Banerjee, S.K. (2000): High-resolution paleomagnetic records from Holocene sediments from the Palmer Deep, western Antarctic Peninsula. Earth Planet. Sci. Lett., **181**, 429–441.

Cande, S.C. and Kent, D.V. (1995): Revised calibration of the geomagnetic polarity timescale for the Late Cretaceous and Cenozoic. J. Geophys. Res., **100**, 6093–6095.

Cande, S.C. and Mutter, J.C. (1982): A revised identification of the oldest sea-floor spreading anomalies between Australia and Antarctica. Earth Planet. Sci. Lett., **58**, 151–160.

Channell, J.E.T., Hodell, D.A. and Lehman, B. (1997): Relative geomagnetic paleointensity and $\delta^{18}O$ at ODP Site 983 (Gardar Drift, North Atlantic) since 350 ka. Earth Planet. Sci. Lett., **153**, 103–118.

Domack, E.W. (1982): Sedimentology of glacial and marine glacial deposits of the George V—Adelie

Continental Shelf, East Antarctica. Boreas, **11**, 79–97.
Eittreim, S.L. and Smith, G.L. (1987): Seismic sequences and their distribution on the Wilkes Land margin. The Antarctic Continental Margin: Geology and Geophysics of Offshore Wilkes Land, ed. by S.L. Eittreim and M.A. Hampton. Houston, Circum-Pacific Council for Energy and Mineral Resources, 15–43 (Earth Sciences Series, v. 5A).
Eittreim, S.L., Cooper, A.K. and Wannesson, J. (1995): Seismic stratigraphic evidence of ice sheet advances on the Wilkes Land margin of Antarctica. Sediment. Geol., **96**, 131–156.
Escutia, C., Warnke, D., Acton, G., Bárcena, M.A., Burckle, L., Canals, M. and Frazee, C.S. (2003): Sediment distribution and sedimentary processes across the Antarctic Wilkes Land Margin during the Quaternary. Deep-Sea Res. II, **50**, 1481–1508.
Florindo, F., Bohaty, S.M, Erwin, P.S., Richter, C., Roberts, A.P., Whalen, P.A. and Whitehead, J.M. (2003): Magnetobiostratigraphic chronology and palaeoenvironmental history of Cenozoic sequences from ODP sites 1165 and 1166, Prydz Bay, Antarctica. Palaeogeogr., Palaeoclimatol., Palaeoecol., **198**, 69–100.
Guyodo, Y., Acton, G.D., Brachfeld, S. and Channell, J.E.T. (2001): A sedimentary paleomagnetic record of the Matuyama chron from the Western Antarctic margin (ODP Site 1101). Earth Planet. Sci. Lett., **191**, 61–74.
Hampton, M.A., Eittreim, S.L. and Richmond, B.M. (1987a): Postbreakup sedimentation on the Wilkes Land Margin, Antarctica. The Antarctic Continental Margin: Geology and Geophysics of Offshore Wilkes Land, ed. by S.L. Eittreim and M.A. Hampton. Houston, Circum-Pacific Council for Energy and Mineral Resources, 75–87 (Earth Sciences Series, v. 5A).
Hampton, M.A., Eittreim, S.L. and Richmond, B.M. (1987b): Geology of sediment cores from the George V continental margin. The Antarctic Continental Margin: Geology and Geophysics of Offshore Wilkes Land, ed. by S.L. Eittreim and M.A. Hampton. Houston, Circum-Pacific Council for Energy and Mineral Resources, 151–174 (Earth Sciences Series, v. 5A).
Hayes, D.E., Frakes, L.A., *et al.* (1975): Initial Rep. Deep Sea Drill. Proj., **28**, 153–177.
Inokuchi, H. and Heider, F. (1992): Magnetostratigraphy of sediments from Sites 748 and 750, Leg 120. Proc. ODP, Sci. Res., **120**, 247–253.
Ishihara, T., Tanahashi, M., Sato, M. and Okuda, Y. (1996): Preliminary report of geophysical and geological surveys of the west Wilkes Land margin. Proc. NIPR Symp. Antarct. Geosci., **9**, 91–108.
Kawai, N., Otofuji, Y. and Kobayashi, K. (1976): Paleomagnetic study of deep-sea sediments using thin sections. J. Geomagn. Geoelectr., **28**, 395–412.
Keating, B. and Sakai, H. (1991): Magnetostratigraphic studies of sediments from site 744, southern Kerguelen Plateau. Proc. ODP, Sci. Res., **119**, 771–794.
Kemp, E.M., Frakes, L.A. and Hayes, D.A. (1975): Paleoclimatic significance of diachronous biogenic facies, Leg 28, Deep Sea Drilling Project. Initial Rep. Deep Sea Drill. Proj., **28**, 909–917.
Lucchi, R.G., Rebesco, M., Busetti, M., Caburlotto, A., Colizza, E. and Fontolan, G. (2002): Sedimentary processes and glacial cycles on the sediment drifts of the Antarctic Peninsula Pacific margin: preliminary results of SEDANO-II project. Antarctica at the Close of a Millennium, Proceedings of the 8th International Symposium on Antarctic Earth Sciences, Wellington, 1999, ed. by J.A. Gamble *et al.* Wellington, The Royal Society of New Zealand, 275–280 (R. Soc. N. Z. Bull., **35**).
Sakai, H. and Keating, B. (1991): Paleomagnetism of Leg 119. Proc. ODP, Sci. Res., **119**, 751–770.
Sakai, H., Funaki, M., Keating, B. and ODP Leg 119 Shipboard Science Party (1990): Paleomagnetic study of ODP Leg 119—Kerguelen Plateau and Prydz Bay. Proc. NIPR Symp. Antarct. Geosci., **4**, 201–212.
Sakai, H., Kikawa, E., Ishihara, T., Kobayashi, H., Komori, K. and Sunagawa, A. (1998): Paleomagnetic study of marine sediments from Antarctic Sea: Central Wilkes Land margin, Dumont d'Urville Sea and Victoria Land Basin. Polar Geosci., **11**, 222–238.
Sagnotti, L., Macr, P., Camerlenghi, A. and Rebesco, M. (2001): Environmental magnetism of Antarctic Late Pleistocene sediments and interhemispheric correlation of climatic events. Earth Planet. Sci. Lett., **192**, 65–80.
Sato, T. and Kobayashi, K. (1989): Long-period secular variations of the earth's magnetic field revealed by Pacific deep-sea sediment cores. J. Geomagn. Geoelectr., **41**, 147–159.
Tanahashi, M., Saki, T., Oikawa, N. and Sato, S. (1987): An interpretation of the multichannel seismic

reflection profiles across the continental margin of the Dumont d'Urville Sea, off Wilkes Land, East Antarctica. The Antarctic Continental Margin: Geology and Geophysics of Offshore Wilkes Land, ed. by S.L. Eittreim and M.A. Hampton. Houston, Circum-Pacific Council for Energy and Mineral Resources, 45–73 (Earth Sciences Series, v. 5A).

Tsumuraya, Y., Tanahashi, M., Saki, T., Machihara, T. and Asakura, N. (1985): Preliminary report of the marine geophysical and geological surveys off Wilkes Land, Antarctica in 1983–1984. Mem. Natl Inst. Polar Res., Spec. Issue, **37**, 48–62.

Veevers, J.J. (1987): The conjugate continental margin of Antarctica and Australia. The Antarctic Continental Margin: Geology and Geophysics of Offshore Wilkes Land, ed. by S.L. Eittreim and M.A. Hampton. Houston, Circum-Pacific Council for Energy and Mineral Resources, 45–73 (Earth Sciences Series, v. 5A).

Weissel, J.K. and Hayes, D.E. (1972): Magnetic anomalies in the Southeast Indian Ocean. Antarctic Oceanology II: The Australian—New Zealand Sector, ed. by D.E. Hayes. Washington, D.C., Am. Geophys. Union, 165–196 (Antarct. Res. Ser., **19**).

Yamazaki, T. (1999): Relative paleointensity of the geomagnetic field during Brunhes Chron recorded in North Pacific deep-sea sediment cores: Orbital influence? Earth Planet. Sci. Lett., **169**, 23–35.